

**Electronic Supplementary Information (ESI) for
“The artificial control of enhanced optical processes in fluorescent molecules
on high-emittance metasurfaces”**

M. Iwanaga,* B. Choi, H. T. Miyazaki, and Y. Sugimoto

National Institute for Materials Science (NIMS), 1-1 Namiki, Tsukuba 305-0044, Japan

*iwanaga.masanobu@nims.go.jp

S1. Sample preparation

To fabricate large-area nanostructured surface structures, namely, metasurfaces, we used UV nanoimprint lithography (NIL). Quartz mold patterns of circular-rod hexagonal array were prepared in advance on a 2-inch-diameter quartz wafer; the patterned areas were set to four $1\times 1\text{ cm}^2$ squares. The mold was imprinted on UV resin that coated silicon-on-insulator (SOI) substrates, the residual thin film was removed by O₂ and N₂ plasma in a well-controlled manner, and the hexagonal-array patterns were transferred to the SOI substrates by a BOSCH process. After removing the resin, Au was deposited by 35 nm; finally, we obtained the stacked complementary (SC) metasurfaces, illustrated in Figure 1a. The procedures including the detailed implemented conditions were already reported [1,2]. We produced tens of the SC metasurfaces in the present experiment. The photographs of the actual samples were presented in the previous papers [1,3,4].

As for setting fluorescence (FL) molecules on the SC metasurfaces, a tiny 2 μL drop of dye solutions of 10 or 50 μM was dispersed on a SC metasurface. The drop uniformly spread out on the SC metasurfaces to an area of 18 mm diameter and became dry promptly; accordingly, we estimated the density of the dispersed molecules to be less than 1 molecule per $15\times 15\text{ nm}^2$. The low density suggests that most of the dispersed FL molecules were isolatedly dispersed; indeed, in the present optical measurement, we did not observe any inhomogeneous optical signals that depend on positions of the laser spot, indicating aggregation of the FL molecules.

As for the molecule density, we note that the molecules involved in the optical data were substantially less than the dispersed density above. This is because the dye molecules are affected by photo-bleaching. In our measurement, the first 3-minute photo-irradiation made emitted optical signals containing Raman and fluorescence to be approximately 1/3, in comparison with the signals at the beginning of photo-irradiation. After the first 3-minute photo-irradiation, the optical signals becomes nearly constant; therefore, we recorded the optical signals for 20 s, which are shown in this paper. Thus, a substantial portion (67%) of the dispersed molecules did not contribute to the optical data shown in this paper. In other words, we measured the optical signals at more sparse density than the dispersed one.

In addition, we once carried out optical measurement using IR783 solution of 2 μM , whose density was 1/25 as compared with the case in Figure 2. Still, the observed signals were similar, in shape, to those in Figure 2. This supports that the measured optical signals come from quite uniformly

dispersed molecules.

Related to the dispersion of molecules, we note that it was difficult to disperse exactly same amount of the dye solutions by using pipette. Roughly speaking, we estimated that 20~30% fluctuations occurred depending on the drops by pipette. Therefore, the measured signal intensities could deviate from the expected ones. However, we stress that the shapes of the measured signals were almost reproduced on each SC metasurface in our measurement. In this sense, we can state reproducibility of the optical signals. A related data appear later (Figure S5).

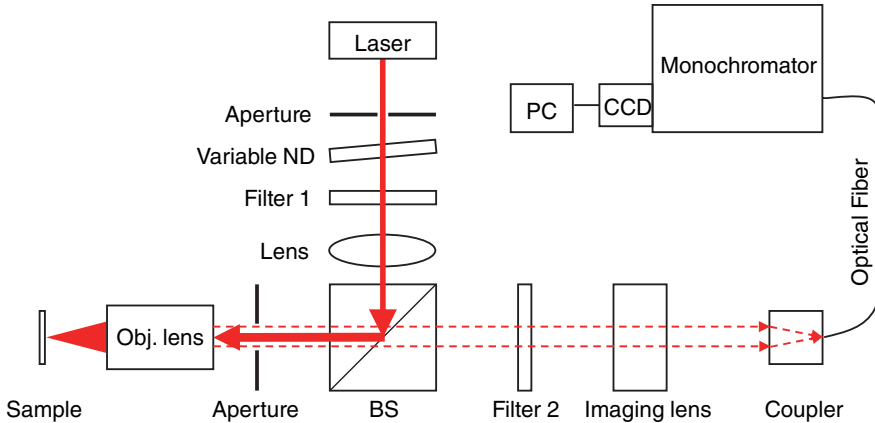


Figure S1. Setup of optical measurement. Both FL and Raman-scattering measurement was carried out in this setup. BS denotes beam splitter, ND neutral density, CCD coupled charge device, and PC personal computer.

S2. Optical measurement

Figure S1 illustrates setup of optical measurement, which was an illumination-collection μ -FL configuration. The illumination and collection were carried out at the normal incidence using an objective lens ($\times 20$) of numerical aperture (NA) 0.4, which was associated with imaging lens. The collected light (or optical signal), represented with red dashed arrows in Figure S1, was coupled to an optical fiber that was connected to a monochromator equipped with a cooled coupled charge device (CCD) camera. The data taking was done by a personal computer (PC).

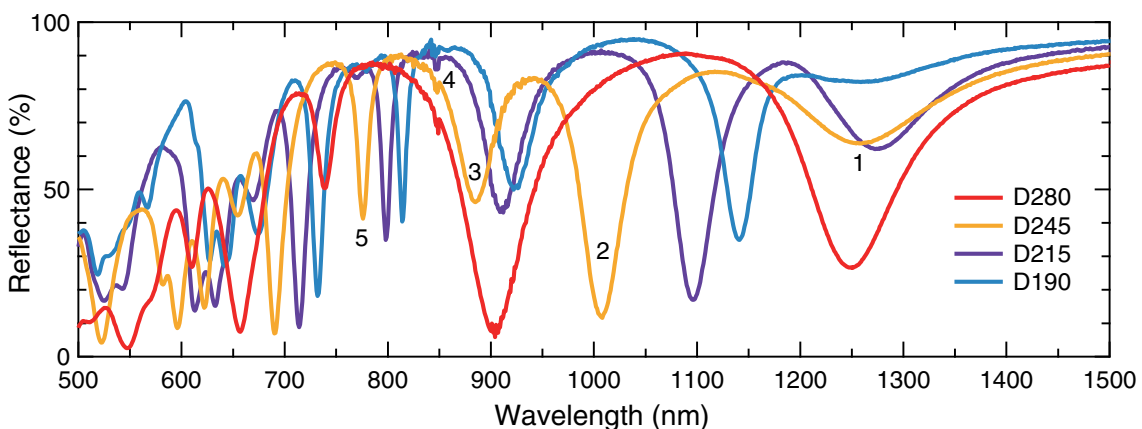


Figure S2. Measured R spectra of SC PlasPh metasurfaces with air-hole diameters D of 190, 215, 245, and 280 nm (light blue, purple, yellow, and red lines, respectively). As for the SC metasurface of D245, the first to fifth resonances are indicated by the numbers from 1 to 5, respectively.

As light sources, single-mode continuous-wave (cw) lasers were used. For IR783 molecules, laser lines of 780.0 or 786.6 nm were used, both of which are on resonance for IR783 molecules. For R590 molecules, a single-mode cw laser of 532.05 nm was used; the wavelength is on resonance for R590 molecules. We note that R590 has been often called R6G in literature because the supplier was different from us. The incident light was focused by the objective lens and the laser-light spots on the samples were typically 25 μm diameter. The laser-light power was typically 2 mW on the SC metasurfaces and kept in the linear response region. The filter 1 in Figure S1 was a laser-line filter to eliminate the side band of the laser lines. The optical signals were accumulated for 20 s on the CCD camera.

Figure S2 shows measured reflectance (R) spectra of the SC metasurfaces with air-hole diameters (D) from 190 to 280 nm. The metasurfaces were not coated by SAM. Light blue, purple, yellow, and red lines denote the R spectra of D190, D215, D245, and D280, respectively. Incident angle was 5° and the polarization was p-polarized, that is, the electric (E)-field vector $\mathbf{E}_{\text{in}} \parallel xz$ plane. The coordinate is shown in Figure 1a. We used a spectrometer for the quantitatively precise R measurement. We note that the R spectra are almost equivalent to the spectra at the normal incidence. The first to fifth resonances of the SC metasurface of D245 are indicated by numbers 1 to 5, respectively. Note that the third and fourth resonances correspond to the numbers 3 and 4 in Figure 2a. We also measured R spectra with varying the incident angles and polarization (not shown here). As a result, we confirmed that the R spectra did not shift so much at the wavelength range of present interest for the incident angles less than 20°; the angle range corresponds to the NA of the objective lens. Thus, the R spectra in Figure S2 are enough to grasp the basic optical properties relevant to this study.

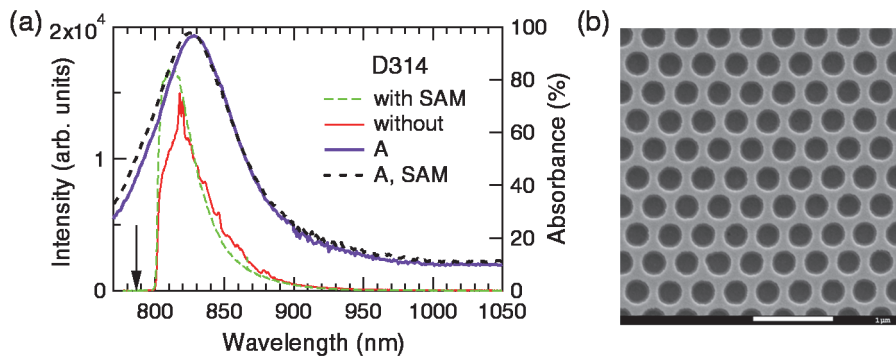


Figure S3. A set of enhanced optical signals from IR783 molecules dispersed on a SC PlasPh metasurface of D314. (a) Enhanced optical signals on the SC metasurfaces without SAM (red line) and with SAM (green dashed line). Purple line denotes A spectrum of the SC metasurface without SAM and black dashed line A spectra with SAM. (b) Top-view SEM image of the SC metasurface of D314. White scale bars in the SEM images indicate 1 μm .

The SC metasurfaces are reflective and therefore absorbance (A) of light can be evaluated using the following equation.

$$A = 100 - R (\%) \quad (i)$$

As noted in the text, transmittance and diffraction are small enough; therefore, they are not included in eqn (i).

Figure S3 shows a set of measured results on enhanced optical signals. The molecules were IR 783. The air-hole diameter D of the SC metasurfaces was 314 nm. We define a simple notation such that the diameter D 314 nm is written as D314. Figure S3a and S3b shows optical spectra and top-view scanning electron microscope (SEM) image of the D314 metasurface, respectively. In the SEM image, the white scale bar indicates 1.0 μ m. The optical spectra in Figure S3a include enhanced signals on the SC metasurfaces with/without SAM; the enhanced spectra are shown with red solid lines representing the case without SAM and those with green dashed lines doing the case with SAM; the corresponding A spectra are shown with black dashed and purple solid lines, respectively.

In Figure S3a, the enhanced spectrum shown with the red line has sharp signals, representing Raman-scattering signals. It is evident that the enhancement of the optical signals takes place at the A peak, which is the second resonance of the SC metasurface. In particular, Raman-scattering signals were highly enhanced in Figure 2a and 2c. Note that the FL spectrum the reference exhibited a simply decreasing profile as wavelength becomes longer (Figure 2g). The Raman band appears at 810–900 nm under the measurement setting. Only FL was observed at the wavelength range longer than 900 nm; since there is not A peak at the range, any prominently enhanced signal was not observed at the range in Figure S3a.

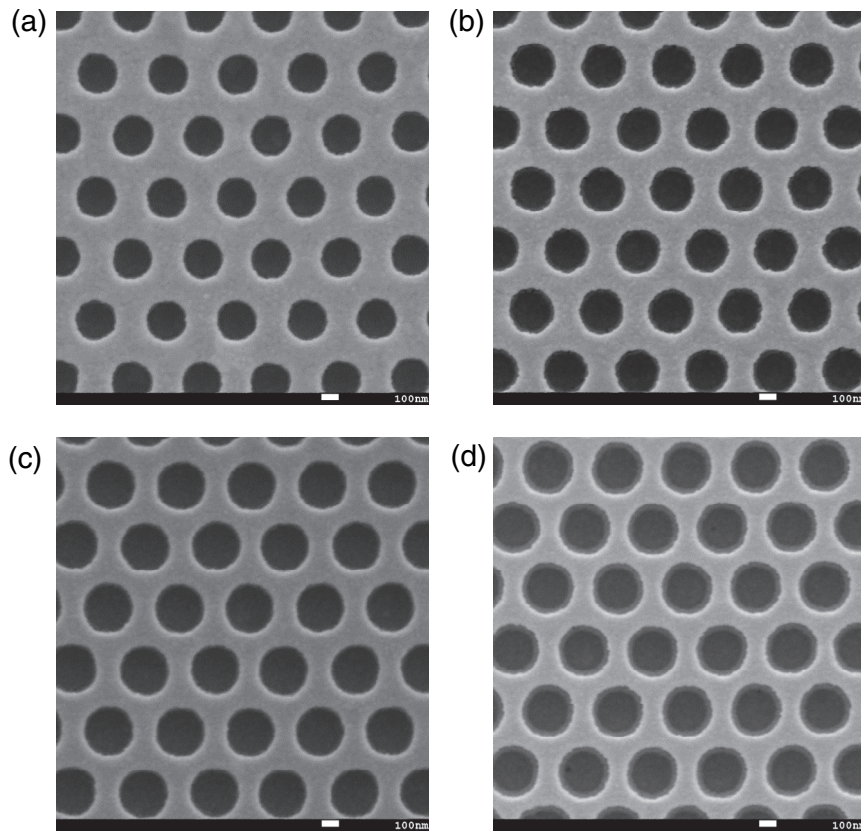


Figure S4. A set of magnified SEM images of the SC metasurfaces. (a) D250 nm. (b) D265 nm. (c) D283 nm. (d) 314 nm. White scale bars indicate 100 nm.

Figure S4 shows a set of SEM images a–d that were taken by magnifying the images in Figure 2b, 2d, 2f, and S3b. These are shown for providing a close look. White scale bars indicates 100 nm. In Figure S4d, the SC metasurface appears to have slight taper inside the holes. The other SC metasurfaces have vertically dug air holes. We note that the spatial resolution of the SEM images is approximately 5 nm, which is mainly determined by the acceleration voltage of 5.0 kV. In addition, there are small fluctuations in the diameters. Therefore, we evaluated averaged values for the SC metasurfaces and determined the diameters such as D250.

Figure S5 presents measured enhanced optical signals of IR783 on two different SC metasurfaces of D250 nm, in order to confirm reproducibility of the spectra. The SC metasurfaces were not covered by a SAM. The dispersed IR783 solutions were nominally 50 μM (red line) and 10 μM (black line). The former is same to the spectrum in Figure 2a. Obviously, the two spectra is quite similar to each other in shape, except for the intensities. Thus, it was confirmed that the reproducibility is quite good. On the other hand, the intensities exhibit quantitative difference from the molar of the dye solution. This is probably because the handing in dispersing the solutions. As is widely known, it is not easy to pick up an exact amount of solution using pipette. We observed at most 20~30% signal-intensity difference on one SC metasurface, due to shot-to-shot change by pipette; therefore, we infer that the deviation from the expected intensity difference comes mainly from the handing. However, we stress that the spot-to-spot measured signal intensities on each SC metasurface were fluctuated only at 5% or less on; in this sense, the measured signals are highly uniform.

Figure S6 shows a sequence of measured results on R590 molecules. Figure S6a show enhanced optical spectra induced by the 532 nm cw laser, whose profile is shown with green line. The spectra are plotted for wavelength in nm. Discrete peaks appear at the FP range, corresponding to the range from 550 to 575 nm. The peaks represent enhanced Raman scattering. The sharp edge at 540 nm comes from the Raman filters that were set at the position of filter 2 in Figure S1 and terminated the strong scattering of the laser light.

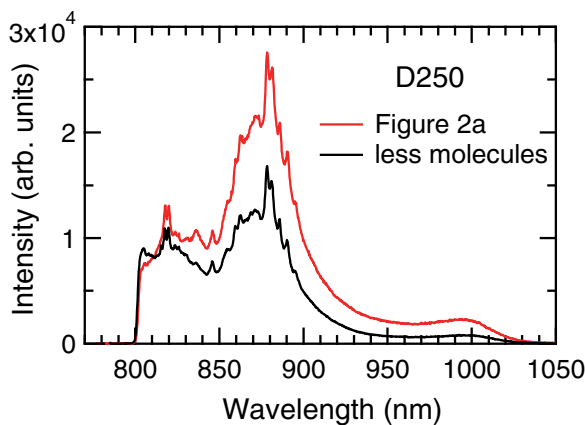


Figure S5. Measured enhanced optical signals of IR783 on two different SC metasurfaces without a SAM. The air-hole diameters were 250 nm. Red line is same to that in Figure 2a. Black line comes from a lower-density IR 783 solution. As for the measuring conditions, they were normalized to each other.

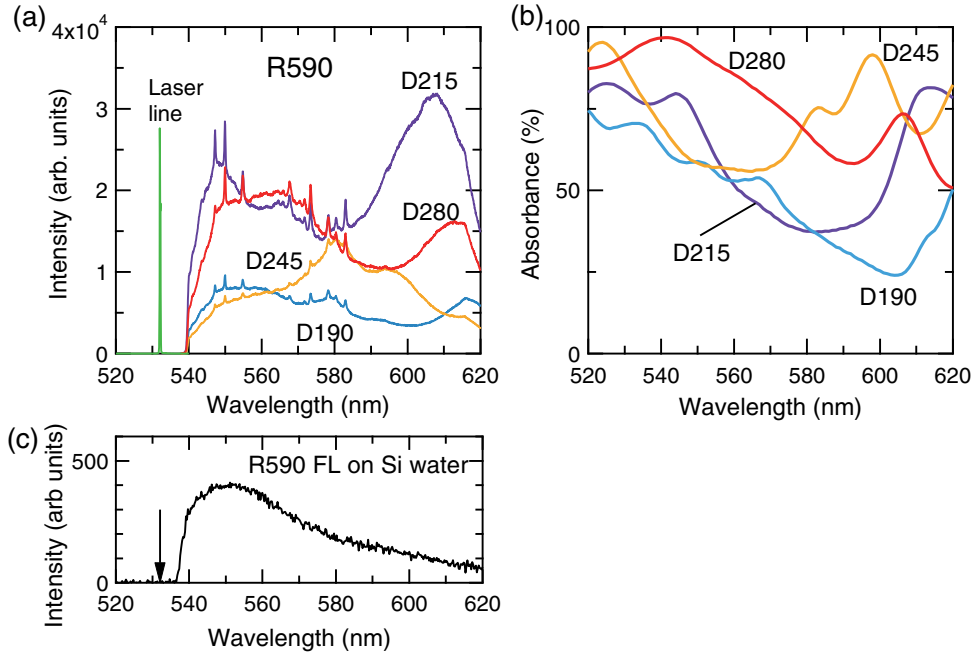


Figure S6. A set of enhanced optical signals from R590 molecules dispersed on the SC PlasPh metasurfaces. (a) Enhanced optical signals from the R590 molecules dispersed on the SC metasurfaces without SAM of D190 (light blue), D245 (yellow), D280 (red), and D215 (purple). (b) Absorbance A spectra of the SC metasurfaces. The diameters, D , are indicated. (c) FL spectrum of R590 molecules dispersed on Si wafer, measured for reference. Arrow indicates the excitation wavelength.

Figure S6b present A spectra, based on measured R spectra and evaluated by eqn (i). The A spectra take rather large values more than 50%. The peaks are related to the enhanced optical signals in Figure S6a. For example, the FL peak at 608 nm in case of D215 is consistent with an A peak at 610 nm in Figure S6b. On the other hand, around 550 nm, the light absorption by constituent materials, Au and Si, themselves increases and does not guarantee the validity of Kirchhoff's radiation law [5]. Therefore, it is difficult to simply relate the A spectra to the enhanced spectra. Still, enhanced optical signals were observed including the FP range.

Figure S6c shows FL spectrum of R590 dispersed on reference Si wafer; the incident laser wavelength is indicated by an arrow. Only FL was dominantly observed. This tendency on the reference circumstance is consistent with that of IR783 in Figure 2. Thus, we confirmed that the FL molecules on the SC metasurfaces keep their FL states and are quite unlikely to be affected on the artificially prepared circumstance.

S3. Numerical details

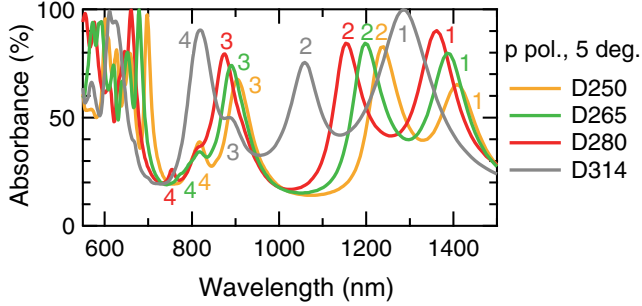


Figure S7. Numerically calculated A spectra of the SC metasurfaces of D250 (yellow), D265 (green), D280 (red), and D314 (gray). Numbers 1 to 4 indicate the first to fourth resonances. Incidence was set to be almost normal to the xy plane and the polarization was in the xz plane. The coordinate is same to that in Figure 1a.

To understand the contributions from resonant electromagnetic (EM) waves on the SC metasurfaces, we implemented numerical calculation with rigorous coupled-wave analysis (RCWA) incorporating scattering (S) matrix method [6,7]. The numerical method is able to compute EM responses solving Maxwell equations numerically and has been well established for periodic structures such as metasurfaces [1–3], metamaterials [8], and photonic crystals [9]. The RCWA and S-matrix code was implemented on supercomputers in a multi-parallel way.

Figure S7 shows computed A spectra of the SC metasurfaces of D250, D265, D280, and D314, which are shown with yellow, green, red, and gray lines, respectively. Incidence traveling in the xz plane was set to be almost normal incidence and the incident angle was set to 5° from the z axis in the coordinate of Figure 1a (or 4c). The polarization was set to be in the xz plane, which is usually called p polarization. Qualitatively, as the diameters of the air holes in the SC metasurfaces become larger, the resonant wavelengths become shorter. This tendency was experimentally confirmed. In this study, we mainly employed the ranges of 800–900 nm for IR 783 and those of 540–600 nm for R590.

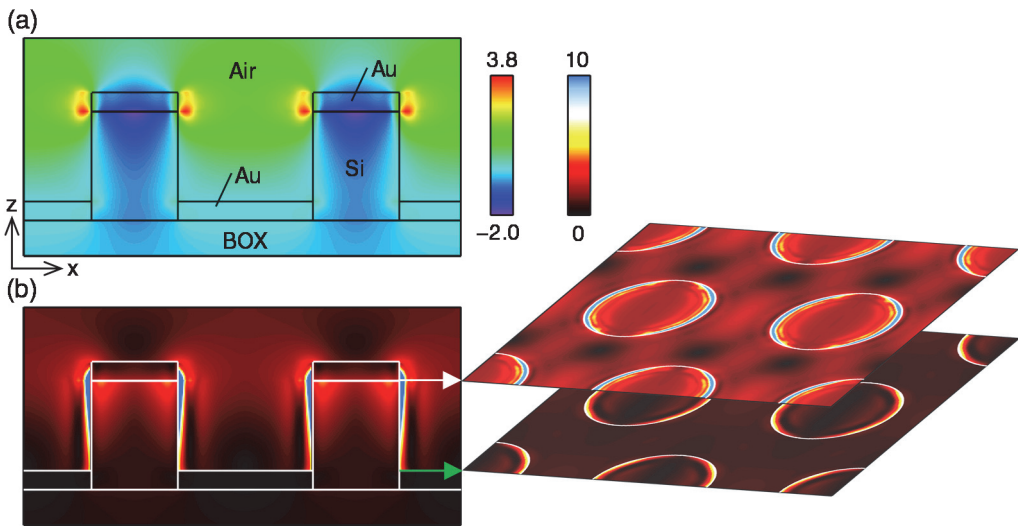


Figure S8. Numerically calculated E-field distribution at the second resonance of 1239.5 nm. (a) Snapshot of E-field distribution at a xz section through the centers of air holes. (b) Absolute value of E field $|E|$, corresponding to (a). Incidence was set to be $|E_{in}|=1.0$ and x -polarized.

Figure S8 shows E-field distributions on the second resonance of the SC metasurface of D250,

which was indicated by the yellow line and the number 2 in Figure 4a. Incidence of wavelength 1239.5 nm in air was set to propagate from the top at the normal incidence. The second resonance also contributed to the enhancement of optical signals (Figure 2). Incidence was set to have the absolute value of $|E_{in}|=1.0$; the polarization was x -polarized in accordance with Figure 4.

Figure S8a shows a snapshot of E_x component in an xz section that is same to that in Figure 4b. Strictly, the plotted E_x is $\text{Re}(E_x)$. The E-field distribution shows that the second resonance is an interface mode between Au and Si; a systematic examination on the resonant modes in the SC metasurface was reported in [3].

Figure S8b displays $|E|$ distribution in an xz section same to Figure S8a and xy sections at the z positions indicated by arrows. The largest $|E|$ values appear at the Au–Si interface of the inner surface of the air holes; the E_z component is mostly responsible for the largest $|E|$. The inner surface of the air holes seems less effective to load the dispersed FL molecules than the Au surfaces at the top and bottom layers; at least, we infer that most of the dispersed molecules are not located at the inner surface. Thus, the largest $|E|$ values unlikely contribute to the enhanced optical signals. The hot spot was not employed in this experiment; instead, we were able to obtain quite uniformly enhanced optical signals. Although the maximum in Figure S8b was 32.0, the panels are displayed at the (0,10) range to grasp the qualitative features.

REFERENCES

- [1] B. Choi, M. Iwanaga, H. T. Miyazaki, K. Sakoda, and Y. Sugimoto, *J. Micro/Nanolithogr. MEMS MOEMS*, 2014, **13**, 023007.
- [2] M. Iwanaga, B. Choi, H. T. Miyazaki, Y. Sugimoto, and K. Sakoda, *J. Nanomater.*, 2015, **2015**, 507656.
- [3] M. Iwanaga and B. Choi, *Nano Lett.*, 2015, **15**, 1904–1910.
- [4] B. Choi, M. Iwanaga, H. T. Miyazaki, Y. Sugimoto, A. Ohtake, and K. Sakoda, *Chem. Commun.*, 2015, **51**, 11470–11473.
- [5] J.-J. Greffet and M. Nieto-Vesperinas, *J. Opt. Soc. Am. A*, 1998, **15**, 2735–2744.
- [6] L. Li, *J. Opt. Soc. Am. A*, 1997, **14**, 2758–2767.
- [7] L. Li, *J. Opt. Soc. Am. A*, 1996, **13**, 1024–1035.
- [8] M. Iwanaga, *Sci. Technol. Adv. Mater.*, 2012, **13**, 053002.
- [9] B. Choi, M. Iwanaga, T. Ochiai, H. T. Miyazaki, Y. Sugimoto, and K. Sakoda, *Appl. Phys. Lett.*, 2014, **105**, 201106.